Neuroscience 141 (2006) 977–988

POSSIBLE SOURCES AND SITES OF ACTION OF THE NITRIC OXIDE INVOLVED IN SYNAPTIC PLASTICITY AT SPINAL LAMINA I PROJECTION NEURONS

R. RUSCHEWEYH,[a] A. GORALCZYK,[a,b] G. WUNDERBALDINGER,[a] A. SCHOBER[b] AND J. SANDKÜHLER[a]*

[a]*Department of Neurophysiology, Center for Brain Research, Medical University of Vienna, Spitalgasse 4, A-1090 Vienna, Austria*

[b]*Neuroanatomy and Interdisciplinary Center for Neurosciences, University of Heidelberg, Im Neuenheimer Feld 307, D-69120 Heidelberg, Germany*

Abstract—The synaptic long-term potentiation between primary afferent C-fibers and spinal lamina I projection neurons is a cellular model for hyperalgesia [Ikeda H, Heinke B, Ruscheweyh R, Sandkühler J (2003) Synaptic plasticity in spinal lamina I projection neurons that mediate hyperalgesia. Science 299:1237–1240]. In lamina I neurons with a projection to the periaqueductal gray, this long-term potentiation is dependent on nitric oxide. In the present study, we used immunohistochemistry to detect possible sources and sites of action of the nitric oxide necessary for the long-term potentiation at lamina I spino-periaqueductal gray neurons in rats. None of the three isoforms of the nitric oxide synthase was expressed in a significant number of lamina I spino-periaqueductal gray neurons or primary afferent C-fibers (as evaluated by staining of their cell bodies in the dorsal root ganglia). However, endothelial and inducible nitric oxide synthase were found throughout the spinal cord vasculature and neuronal nitric oxide synthase was present in a number of neurons in laminae II and III. The nitric oxide target soluble guanylyl cyclase was detected in most lamina I spino-periaqueductal gray neurons and in approximately 12% of the dorsal root ganglion neurons, all of them nociceptive as evaluated by coexpression of substance P. Synthesis of cyclic 3′,5′-guanosine monophosphate upon stimulation by a nitric oxide donor confirmed the presence of active guanylyl cyclase in at least a portion of the spino-periaqueductal gray neuronal cell bodies. We therefore propose that nitric oxide generated in neighboring neurons or blood vessels acts on the spino-periaqueductal gray neuron and/or the primary afferent C-fiber to enable long-term potentiation. Lamina I spino-parabrachial neurons were stained for comparison and yielded similar results. © 2006 IBRO. Published by Elsevier Ltd. All rights reserved.

Key words: nociception, spinal cord, dorsal root ganglion, soluble guanylyl cyclase, C-fiber.

*Corresponding author. Tel: +43-1-4277-628-35; fax: +43-1-4277-628-65.
E-mail address: juergen.sandkuehler@meduniwien.ac.at (J. Sandkühler).

Abbreviations: cGMP, cyclic 3′,5′-guanosine monophosphate; CTX-B, cholera toxin subunit B; DRG, dorsal root ganglion; eNOS, endothelial nitric oxide synthase; IBMX, isobutylmethylxanthine; iNOS, inducible nitric oxide synthase; ir, immunoreactivity; LTP, long-term potentiation; NDS, normal donkey serum; NK1 receptor, neurokinin 1 receptor; nNOS, neuronal nitric oxide synthase; NO, nitric oxide; NOS, nitric oxide synthase; PAG, periaqueductal gray; PB, 0.1 M phosphate buffer, pH 7.4; PBS, 0.1 M phosphate-buffered saline, pH 7.4; sGC, soluble guanylyl cyclase; SNAP, S-nitroso-N-acetyl-D,L-penicillamine; SP, substance P.

The gaseous molecule nitric oxide (NO) is a cell-permeant neuromodulator that is synthesized on demand by the enzyme nitric oxide synthase (NOS). Binding of NO to its main target molecule, soluble guanylyl cyclase (sGC), induces formation of cyclic 3′,5′-guanosine monophosphate (cGMP) which activates several intracellular pathways (Esplugues, 2002). NO modulates nociception at different levels of the neuraxis (see literature in Meller and Gebhart, 1993 and Hoheisel et al., 2005). In the spinal cord, both hyperalgesic and analgesic effects of NO are discussed (Hoheisel et al., 2005). A number of studies report spinal NO to be necessary for the expression of thermal hyperalgesia in animal models of long-lasting pain, but not for acute nociception (Meller and Gebhart, 1993; Osborne and Coderre, 1999).

A similar significance for long-lasting pain has been attributed to spinal lamina I neurons that express the neurokinin 1 (NK1) receptor, many of which have a projection to the brainstem, e.g. the periaqueductal gray (PAG) and the parabrachial area (Ding et al., 1995; Todd et al., 2000). Selective ablation of these neurons prevents the expression of full hyperalgesia in rat models of inflammatory and neuropathic pain, but does not affect the responses to acute noxious stimuli (Mantyh et al., 1997; Nichols et al., 1999; Khasabov et al., 2002).

We recently found a possible link between NO and lamina I projection neurons in the generation of long-lasting pain. Synaptic long-term potentiation (LTP) at nociceptive spinal synapses is a cellular model for centrally mediated hyperalgesia (Sandkühler, 2000). Consistently, LTP can be induced at synapses between primary afferent C-fibers, many of which are nociceptive, and lamina I projection neurons, but not lamina I interneurons (Ikeda et al., 2003). We have recently shown that LTP in spino-PAG neurons is dependent on synthesis of NO, its diffusion through the extracellular space and its action on sGC (Ikeda et al., in press).

The aim of the present study was to detect possible sources and sites of action of the NO necessary for the LTP at the synapse between primary afferent C-fibers and lamina I spino-PAG neurons. NO diffuses freely through cell membranes and thus can reach neurons and other cells that lie within about 100 μm from its source (Wood and Garthwaite, 1994). It could for example be synthesized in the primary afferent and diffuse to its target in the projection neuron, as in classical anterograde transmission. Alternatively, it could be generated in the projection neuron and diffuse to the primary afferent terminal to reach its target. NO acting in this way, as a retrograde transmit-

0306-4522/06$30.00+0.00
doi:10.1016/j.neuroscience.2006.04.010

ter, is involved in hippocampal LTP (Hawkins et al., 1998). As a third possibility, NO might be produced in neighboring interneurons or another type of cell and diffuse to either the primary afferent terminal or the lamina I projection neuron to find its target. E.g., in cerebellar LTD, NO produced by nearby interneurons seems to act on the postsynaptic cell (Daniel et al., 1998). We used immunohistochemistry to detect the NO synthesizing enzyme NOS and the NO target sGC in lamina I projection neurons, primary afferents and neighboring spinal cells. Presence of active sGC was confirmed by evaluating cGMP synthesis in response to an NO donor. Not only the neuronal isoform of nitric oxide synthase (nNOS), but also the endothelial and inducible isoforms (eNOS and iNOS) have been implicated in LTP induction (Hawkins et al., 1998; Constantine-Paton and Cline, 1998; Ikeda and Murase, 2004), and therefore antibodies against each of these isoforms were used.

EXPERIMENTAL PROCEDURES

Retrograde labeling of lamina I projection neurons

All procedures used were in accordance with European Communities Council directives (86/609/EEC) and were approved by the Austrian Federal Ministry for Education, Science and Culture. Every effort was made to minimize the number of animals used and their suffering. Stereotaxic injections into the brain were performed in 22 young (18–24 day-old) Sprague–Dawley rats as previously described (Ikeda et al., 2003; Ruscheweyh et al., 2004). Briefly, rats were anesthetized with a mixture of ketamine and xylazine (75 mg kg^{-1} and 7.5 mg kg^{-1} i.p., respectively) and placed in a stereotaxic apparatus. A small scalp cut (<1 cm) was made and a hole was drilled into the skull bone to allow insertion of the needle of a 500 nl Hamilton syringe (Hamilton AG, Bonaduz, Switzerland) into the targeted area. The animals received a single injection of one of the retrograde tracers (CM-DiI, 1.25%, 50–100 nl, Molecular Probes, Eugene, OR, USA or fluorogold, 5%, 25–50 nl, Fluorochrome, Denver, CO, USA or cholera toxin subunit B, CTX-B, 0.5%, 80–180 nl, Research Biochemicals International, Natick, MA, USA) into the right caudal and/or intermediate part of both the lateral and ventrolateral PAG, or, for comparison, into the right lateral parabrachial area, according to the coordinates obtained from the atlas of Swanson (1992). The use of different tracers was necessary because CM-DiI was not stable following certain pre-treatments necessary for immunohistochemistry. In addition, the fluorescence of fluorogold was too unstable to allow identification of double labeling in projection neurons so that fluorogold and CTX-B had to be detected with antibodies that could not be combined with every type of immunohistochemistry.

The head wound was closed with two stitches and subsequent daily inspection revealed no signs of infection. After recovery from anesthesia, the animals fed and drank normally and no pain-related behavior was observed. Three to four days after tracer injection, the spinal cord and/or the dorsal root ganglia (DRGs) were removed under anesthesia and processed for histochemistry as described below. The brain was excised, frozen in isopentane at −20 °C and 20 μm thick cryosections were obtained to allow histological verification of the injection site. While injection sites of CM-DiI and fluorogold could be directly examined by fluorescence microscopy, CTX-B injection sites had to be detected by immunohistochemical methods as described below. Only animals where the injection site was clearly confined to either the parabrachial area or the PAG were included in the present study. Examples of equivalent injection sites that illustrate the spread of the tracer can be found in our previous papers (Ikeda et al., 2003; Ruscheweyh et al., 2004; Dahlhaus et al., 2005).

Pre-treatment of tissue for immunostaining and NADPH diaphorase histochemistry

Lumbar segments 4–6 of the spinal cord and corresponding DRGs were obtained from 30 young (21–28 day-old) Sprague–Dawley rats (22 tracer-injected and eight untreated animals) and pretreated as follows. The plane of cutting was transversal for spinal cord and arbitrary for DRGs.

Pre-treatment for immunostaining for eNOS and iNOS. After killing the rat by an overdose of ketamine/xylazine, spinal cord and/or DRGs were removed without prior fixation and immediately snap frozen in isopentane at −80 °C. Ten micrometer thick sections were cut on a cryomicrotome (Leica CM 3050, Nussloch, Germany) and mounted onto glass slides.

Pre-treatment for sGCβ1 (antibody #2, see below), substance P (SP), nNOS and fluorogold immunohistochemistry and NADPH diaphorase staining. Under deep anesthesia with ketamine/xylazine, rats were transcardially perfused with cold (4 °C) 0.9% NaCl followed by freshly prepared cold 2% paraformaldehyde in 0.1 M phosphate buffer, pH 7.4 (PB). Spinal cord and/or DRGs were removed and stored in the same fixative for one hour. Tissue was cryoprotected in 20% sucrose in PB overnight, then snap frozen and cryosections were obtained as described above.

Pre-treatment for sGCβ_1 (antibody #1, see below) and CTX-B immunohistochemistry. Rats were perfused and spinal cords/DRGs postfixed as described above, then 20–30 μm thick sections were cut on a vibratome (DSK Microslicer DTK-1000, Osaka, Japan).

Activation of sGC and pre-treatment for cGMP immunohistochemistry. The procedures used were similar to the cGMP detection protocols described in Vles et al. (2000). Rats that had 3–4 days previously received an injection of CM-DiI into the PAG or parabrachial area were killed by decapitation under deep isoflurane anesthesia, the lumbar spinal cord was removed and transverse, 500 μm thick slices were cut on a vibratome and collected in incubation solution that consisted of (in mM): NaCl 124, KCl 5, KH_2PO_4 1.3, $CaCl_2$ 2.4, $MgSO_4$ 1.3, $NaHCO_3$ 26, glucose 15, equilibrated with 95% O_2 and 5% CO_2. Slices were then preincubated in recording solution (identical to the incubation solution except for (in mM) NaCl 127, KCl 1.9 and $CaCl_2$ 4.3) containing 1 mM isobutylmethylxanthine (IBMX, Sigma-Aldrich) for 30 min to inhibit phosphodiesterase activity. This was followed by a 10 min exposure to the NO-donor S-nitroso-N-acetyl-D,L-penicillamine (SNAP, 200 μM, Alexis, Grünstadt, Germany) in the continued presence of IBMX. The whole procedure was conducted at 37 °C. Next, slices were fixed in cold 4% paraformaldehyde in PB for 2 h, followed by overnight storage in 20% sucrose in PB. Slices were then snap frozen and 8 μm thick cryosections were obtained.

Immunostaining and NADPH diaphorase histochemistry procedures

Unless otherwise indicated, 0.1 M phosphate buffered saline, pH 7.4 (PBS), was used for washing of sections between incubation steps, for diluting antibodies to working concentrations and for preparation of blocking media. Two different antibodies against sGCβ_1 were used and designated as #1 and #2. Secondary antibodies were applied for one hour. Please refer to the previous subsection for fixation and further pre-treatment of the tissue. Omission of the primary antibody abolished staining in every case. Double and triple stainings showed no cross-reactions when one of the primary antibodies was omitted. No or very weak bleed-through across different filters was seen when one set of primary and secondary antibody was omitted from the double or triple stainings. This weak bleed-through was clearly different from staining judged to be positive.

Double staining for sGCβ_1 and CTX-B (spinal cord). Free floating vibratome sections were permeabilized with 50% ethanol for 30 min, then treated with 3% H_2O_2 for 30 min followed by 5% normal donkey serum (NDS) for 15 min. Goat anti-CTX-B (1:2000, Biotrend 2060-0004, Köln, Germany) in 1% NDS was applied overnight at 4 °C and then visualized with Cy3-coupled anti-goat IgG (1:100, Jackson Immunoresearch Laboratories, West Grove, PA, USA), followed by rabbit anti-sGCβ_1 #1 (1:50, provided by H. H. H. W. Schmidt, Gieβen, Germany, characterized in Zabel et al., 1998, 1999) in 5% NDS overnight at 4 °C and then biotin-coupled anti-rabbit IgG (1:300, Amersham, Buckinghamshire, UK). Sections were incubated with Cy2-conjugated streptavidin (1:100, Jackson Immunoresearch), mounted onto glass slides and coverslipped.

For surveys of sGCβ_1 staining in the absence of CTX-B, sGCβ_1 was visualized by horseradish peroxidase-conjugated streptavidin (1:100, Amersham) followed by diaminobenzidine solution (6 mg diaminobenzidine (Fluka, Buchs, Switzerland) and 0.1 ml 3% H_2O_2 in 10 ml PBS).

Double staining for nNOS and fluorogold (spinal cord). Cryosections were incubated with mouse anti-nNOS (1:500, Sigma-Aldrich N2280, St. Louis, MO, USA) and rabbit anti-fluorogold (1:200, Fluorochrome, Denver, CO, USA) overnight at 4 °C. Immunostaining was visualized by FITC-coupled anti-mouse IgG (1:400, Chemicon, Temecula, CA, USA) and Cy3-coupled anti-rabbit IgG (1:200, Jackson Immunoreseach), respectively.

Double staining for nNOS or sGCβ_1 and NeuN (spinal cord). Sections were stained for nNOS or sGCβ_1 (antibody #1) as described above, followed by incubation in mouse anti-NeuN (1:500, Chemicon MAB377) in 5% NDS for one hour and visualization by Cy3-coupled anti-mouse IgG (1:200, Chemicon).

Double staining for sGCβ_1 and NeuN (DRG). Cryosections were incubated overnight with rabbit anti-sGCβ_1 #2 (1:1000, Cayman Chemicals 160897, Ann Arbor, MI, USA) in 5% NDS and 0.1% Triton X-100 followed by Cy3-coupled anti-rabbit IgG (1:200). Then mouse anti-NeuN (1:500) in 5% NDS was applied for one hour and visualized by FITC-coupled anti-mouse IgG (1:400).

Triple staining for nNOS, SP and NeuN (DRG). nNOS and SP were simultaneously stained by incubating cryosections overnight in mouse anti-nNOS (1:500) and rabbit anti-SP (1:2000, Diasorin 20064, Stillwater, MN, USA) in 5% NDS and 0.1% Triton X-100, followed by FITC-coupled anti-mouse IgG (1:400) and Cy5-coupled anti-rabbit IgG (1:100, Chemicon). NeuN was visualized by application of mouse anti-NeuN antibody (1:500) in 5% NDS for 1 h followed by Cy3-coupled anti-mouse IgG (1:200).

Colocalization of sGCβ_1 (antibody #2) and SP (DRG). While colocalization of most antigens was determined by double labeling, this was not possible in the case of sGCβ_1 and SP, because both primary antibodies were raised in the same species. Therefore we performed single sGCβ_1 and SP stainings using the protocols described above and visualizing by Cy3-coupled anti-rabbit IgG (1:200) and Cy2-coupled anti-rabbit IgG (1:50, Jackson Immunoresearch), respectively, on adjacent 3 μm sections. Corresponding cells could easily be detected in the adjacent sections according to their location and morphology.

eNOS (spinal cord, DRG). Cryosections were postfixed in acetone for 10 min at −20 °C, followed by 4% paraformaldehyde in 0.1 M PB for 10 min at room temperature, washed, blocked in 5% NDS and 0.3% Triton X-100 for 2 h and incubated overnight with mouse anti-eNOS (1:10,000, BD Transduction Laboratories 610296, San Jose, CA, USA) in the same blocking solution. Cy3-coupled anti-mouse IgG (1:200) was used for visualization. This protocol was similar to that used by Töpel et al. (1998). For direct comparison with the results of Henrich et al. (2002), we additionally stained 10 μm-cryosections of immersion-fixed (4% paraformaldehyde/0.2% picric acid in 0.1 M PB) DRGs with the same eNOS antibody at 1:160 and 1:1000 dilutions.

iNOS (spinal cord, DRG). Cryosections were incubated overnight in rabbit anti-iNOS (1:100, BD Transduction Laboratories 610332) in 5% NDS and 0.1% Triton X-100, followed by Cy3-coupled anti-rabbit IgG (1:200).

cGMP (spinal cord). Cryosections were incubated overnight with sheep anti-cGMP (1:5000, provided by J. de Vente, Maastricht, The Netherlands, characterized in Tanaka et al. (1997) and de Vente et al. (1998)) in 5% NDS and 0.1% Triton X-100, followed by Cy2-coupled anti-sheep IgG (1:200, Jackson Immunoresearch).

After immunostaining, sections were coverslipped in a glycerine-based antifading medium, containing Mowiol (Hoechst, Germany) and propyl gallate (Sigma-Aldrich).

NADPH-diaphorase staining (spinal cord). Ten micrometer cryosections were incubated for 1 h at 37 °C in the reaction medium, consisting of 0.1 mg/ml nitroblue tetrazoliumchloride, 1 mg/ml NADPH (both Serva, Heidelberg, Germany) and 0.3% Triton X-100 in 0.1 M PB, pH 7.4. After washing with PB, sections were dehydrated and coverslipped in DePeX (Serva).

Data acquisition and analysis

Sections were examined with an Olympus (Tokyo, Japan) microscope under epifluorescence illumination using the appropriate filter sets to identify labeled neurons. Fluorescence images were acquired with a CCD camera (Olympus DP50). AnalySIS software (Soft Imaging Systems, Münster, Germany) was used for image acquisition and measurements. For the purpose of the present study, exact quantification of the percentage of double-labeled neurons was not necessary. Therefore, profile counts were used to estimate the number of stained neurons. Retrogradely labeled spinal lamina I neurons with a projection to the PAG or the parabrachial area were examined in terms of their expression of nNOS, sGCβ_1 or cGMP. The entire L4–L6 segment of every animal was used for counting, but sections were spaced 50 μm to avoid double counting of the large projection neurons. Numbers of counted projection neurons were lower for the sGCβ_1 staining because some of the sections were damaged during the repeated transfers necessary in the course of the free-floating staining procedure. Numbers were also lower for cGMP staining because this required re-sectioning of the 500 μm vibratome slices. To estimate the proportion of lamina I neurons expressing sGCβ_1 or nNOS, the number of sGCβ_1- or nNOS-positive neurons was compared with the number of NeuN-expressing neurons, where all neurons lying within a distance of approximately 25 μm from the dorsal overlying white matter were considered to belong to lamina I. This corresponded to the zone where the tangential orientation of the neuropil typical of lamina I was seen and where the projection neurons, that are largely absent from lamina II, were found. Only neurons with a nucleus visible in the NeuN staining were counted. Here, 200–300 neurons/animal were considered sufficient and a corresponding number of sections was evaluated. In DRGs, the size of cells was determined by calculating the mean of the largest diameter and the diameter perpendicular to it. Only cells with nucleoli clearly visible in the NeuN staining were analyzed. Also here, sections were spaced 50 μm to avoid double counting of neurons. All reasonably large DRG sections from one animal were used for the evaluation of nNOS expression because of its low incidence but only a part of the sections was evaluated for sGC staining that had a higher incidence.

All values are means±S.E.M. The non-parametric Mann-Whitney rank-sum test was used for statistical comparison.

RESULTS

Scarce nNOS immunoreactivity (ir) in spinal lamina I projection and interneurons

nNOS immunostaining in the superficial dorsal horn exhibited a characteristic bilaminar pattern with prominent fiber labeling in laminae I and III (Fig. 1A). Small stained neurons were mainly seen in laminae II and III. The proportion of lamina I neurons showing nNOS-ir was estimated by costaining with the neuronal marker NeuN, and we found that 1–3% of the lamina I neurons exhibited somatic nNOS-ir (302 and 324 cells inspected per animal, $n=2$ rats). Similarly, the expression of nNOS in lamina I spino-PAG neurons was very low (Fig. 1A; Fig. 1B–D shows one of the scarce nNOS-ir spino-PAG neurons, 1±1%, 75–129 cells studied per animal, $n=3$ rats). This result was confirmed by NADPH diaphorase staining (0±0%, 27–86 cells studied per animal, $n=3$ rats). Throughout this study, lamina I neurons with a projection to another brainstem region, the parabrachial area, were studied for comparison. Similar to spino-PAG neurons, spino-parabrachial neurons rarely showed nNOS expression (nNOS-ir: 1±0%, 113–216 neurons studied per animal, $n=3$ rats; NADPH diaphorase staining: 1±0%, 82–212 neurons studied per animal, $n=3$ rats).

Lack of eNOS and iNOS-ir in spinal dorsal horn neurons

eNOS-ir was visible exclusively in the endothelial lining of blood vessels throughout the gray and white matter of the spinal cord (Fig. 2A,B). No iNOS-ir was detected in spinal cord with standard perfusion and fixation protocols as de-

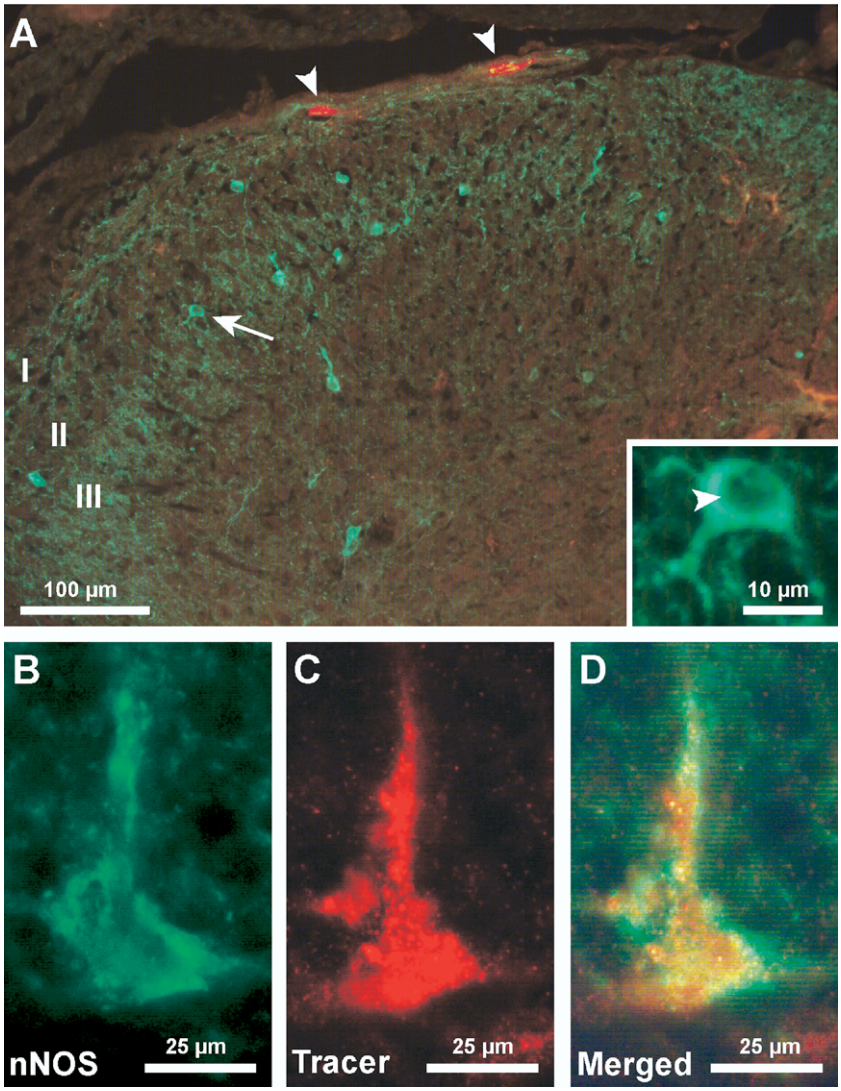

Fig. 1. nNOS in spinal dorsal horn and lamina I projection neurons. (A) nNOS staining (green) of the dorsal horn revealed the typical bilaminar pattern with dense fiber plexus in laminae I and III and scattered small neuronal somata, mainly in laminae II and III. The two lamina I neurons retrogradely labeled from the PAG with fluorogold (red, arrowheads) do not show nNOS-ir. The neuron marked with an arrow is magnified in the inset and illustrates the typical cytoplasmic nNOS staining pattern where the nucleus (arrowhead) remains unstained. Roman numbers indicate approximate location of laminae I–III. B–D show one of the scarce nNOS-positive spino-PAG neurons. Tracer: fluorogold.

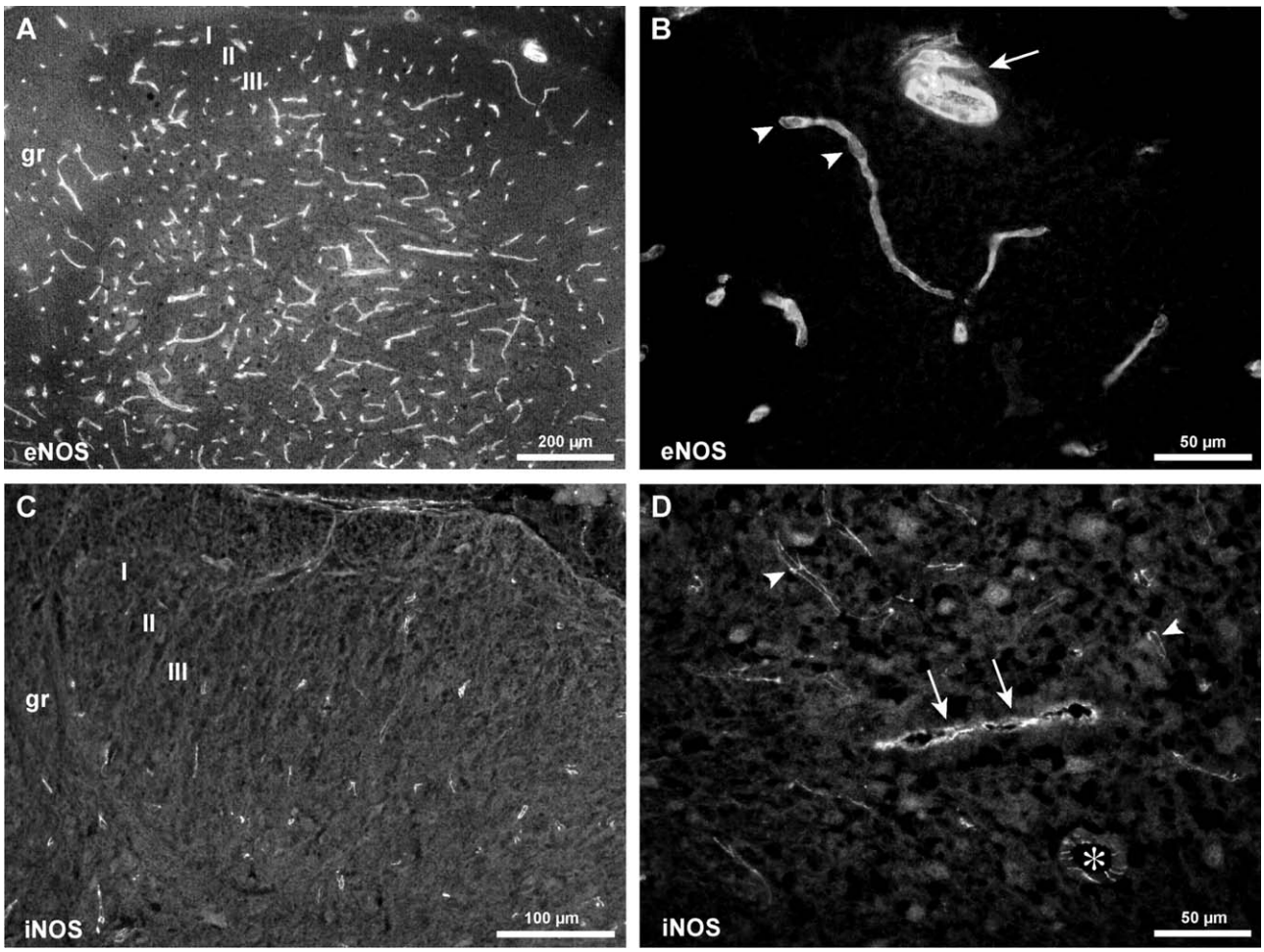

Fig. 2. eNOS and iNOS in spinal dorsal horn. A shows eNOS staining in an overview of the dorsal horn. The endothelial lining of the gray and white matter vasculature is immunopositive, but neuronal structures are not labeled. B shows an enlargement of the superficial dorsal horn. Arrow, transversally cut arteriole; arrowheads, nuclei of capillary endothelium. (C, D) iNOS is found only in laminar, vasculature-associated structures and in the lining of the central canal. (C) Overview of the dorsal horn, (D) enlargement of the region around the central canal (arrows). Arrowheads, laminar vasculature-associated iNOS-ir; asterisk, iNOS-ir in the wall of an arteriole. Roman numbers indicate approximate location of laminae I–III; gr, fasciculus gracilis.

scribed in Hu et al. (2000) and Maihöfner et al. (2000). However, preliminary experiments had shown that in thymus, which was used as a control tissue because of its high iNOS expression, the best iNOS staining was obtained using unfixed material. With this protocol, iNOS-ir was encountered in laminar structures apparently associated with the vasculature and the lining of the central canal (Fig. 2C, D). The exact nature of these laminar structures was not further investigated. No iNOS-ir was found in spinal neurons.

Many lamina I neurons, especially projection neurons, exhibit sGCβ_1-ir

When the sGCβ_1 antibody #2 was used, no neuronal structures were labeled in the spinal cord (not shown). In contrast, with antibody #1, numerous neurons throughout all spinal cord laminae, including large motoneurons, exhibited sGCβ_1-ir (Fig. 3A). In superficial dorsal horn, a dense plexus of sGCβ_1-positive processes was seen, and sGCβ_1-ir was detected in many small and some larger neuronal somata without a clear laminar preference (Fig. 3B). The proportion of lamina I neurons expressing sGCβ_1 was estimated by double labeling with NeuN and amounted to 53±3% (183–254 cells inspected per animal, $n=3$ rats). sGCβ_1 was also frequently encountered in spino-PAG neurons (89±4%, 14–50 neurons examined per animal, $n=3$ rats, Fig. 3D–F) and spino-parabrachial neurons (81±4%, 16–82 neurons examined per animal, $n=4$ rats, $P=0.23$ for comparison with spino-PAG neurons).

cGMP synthesis in lamina I projection neurons

Acute spinal cord transverse slice preparations were used in these experiments. Application of the NO-donor SNAP (200 μM) in the presence of the phosphodiesterase inhibitor IBMX (1 mM) induced extensive cGMP-ir in superficial dorsal horn neurons and neuronal processes (Fig. 3C). In total, 35±6% of the spino-PAG neurons and 23±2% of the

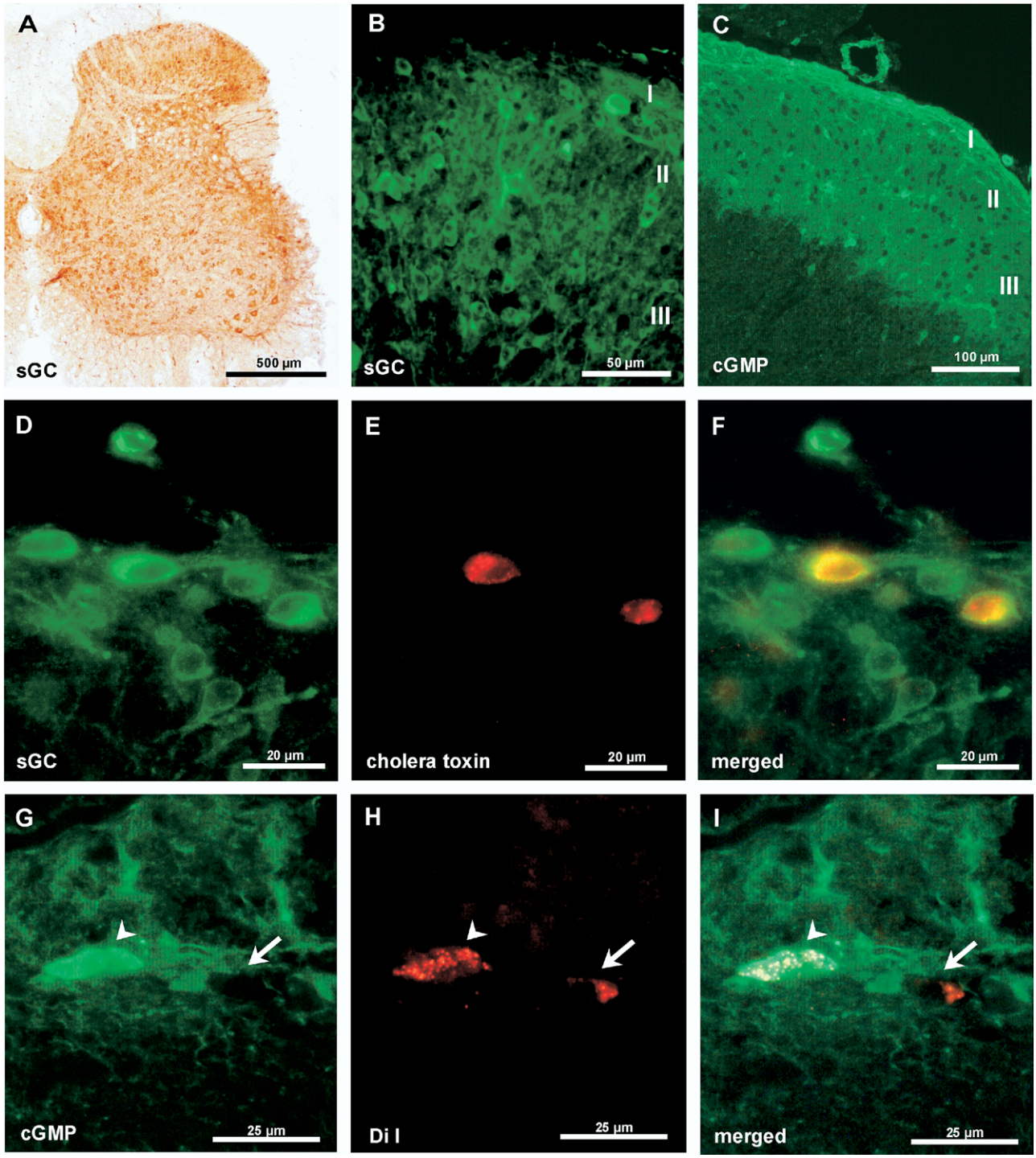

Fig. 3. sGCβ_1 and cGMP in spinal cord and lamina I projection neurons. (A) The spinal cord overview shows that sGCβ_1-ir, here visualized by DAB, is present in neurons and fibers throughout the spinal gray matter, including large motoneurons. (B) A dense sGCβ_1-ir fiber plexus and many immunoreactive neurons are present in the superficial dorsal horn. (C) After stimulation with the NO-donor SNAP, dense cGMP-ir is seen in fibers and neurons in laminae I–III. Roman numbers indicate approximate location of laminae. D–I illustrate sGCβ_1 and cGMP-ir in lamina I projection neurons. Two neurons retrogradely labeled from the PAG with CTX-B (D, red) show sGCβ_1-ir (C, green) and appear yellow in the overlay (E). Arrowhead and arrow indicate two neurons retrogradely labeled from the parabrachial area by DiI (H, red). The neuron marked by the arrowhead shows cGMP-ir (G, green) and appears yellow in the overlay (I) while the neuron marked by the arrow lacks cGMP.

spino-parabrachial neurons in lamina I showed somatic cGMP-ir after this treatment (33–63 neurons examined per animal, $n=4$–5 rats, difference not significant with $P=0.19$, Fig. 3G–I).

Scarce NOS-ir in DRG neurons

Few nNOS-ir neurons were present in lumbar DRGs (0.7%, 1341–1776 cells evaluated per animal, $n=3$ rats, Fig. 4A). The majority of these neurons were small (diameter 23 ± 1 μm, $n=32$ cells, corresponding to the total number of nNOS-ir neurons found in the three rats) and all of them showed SP-ir (Fig. 4A–C).

Using the same protocol as for the spinal cord staining, eNOS-ir was restricted to vascular elements in DRG sections (Fig. 4D). No satellite cells or neurons exhibited eNOS-ir. In contrast, Henrich and co-workers (2002), using the same antibody, reported dot-like eNOS-ir in every DRG neuron. Using their protocol, we could see some dot-like staining, that was, however, not clearly correlated with the cytoplasm of a given neuron and not very different from the background fluorescence. The vascular eNOS staining clearly stood out against a low background using the eNOS antibody at a dilution of 1:10,000, but the dot-like staining started to become visible only at a dilution of 1:1000. Taken together, with our methods, we

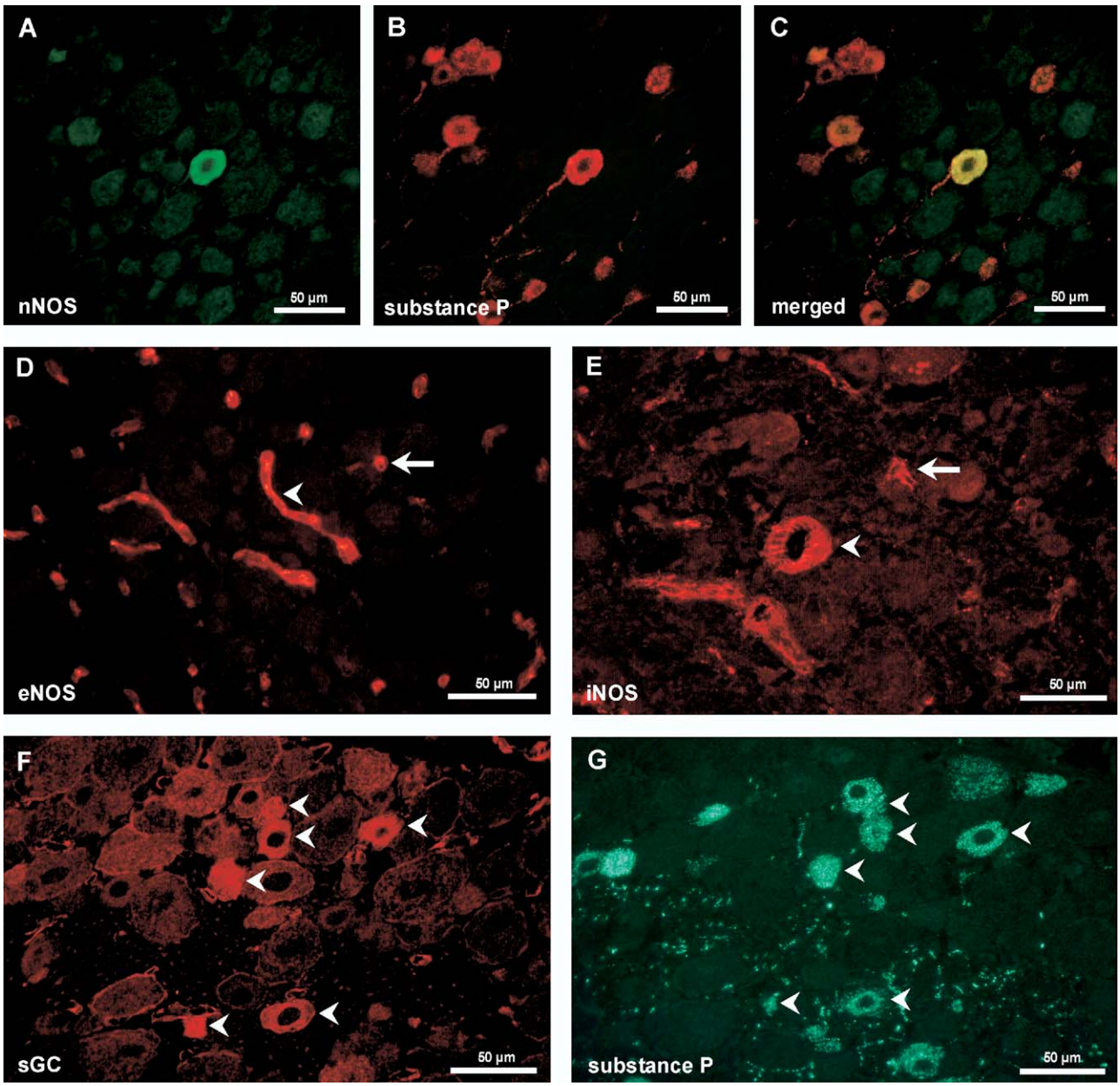

Fig. 4. NOS and sGCβ_1 immunoreactivities in DRGs. (A–C) Only occasional nNOS-positive neurons were found in the DRGs and all of them also showed SP-ir. (D) eNOS was confined to the vascular endothelium. Arrowhead, longitudinally cut capillary; arrow, transversally cut capillary. (E) As in the spinal cord, iNOS was limited to laminar vasculature-associated structures. Arrowhead, laminar, probably capillary-associated structure; arrow, arteriole. (F) sGCβ_1 was expressed by satellite cells and also by a significant proportion of DRG neurons (arrowheads). Colocalization of sGCβ_1-ir with SP-ir was determined on adjacent slices (G) so that the neuronal shape slightly differs between F and G. Arrowheads point to corresponding cells in F and G, showing that colocalization of SP and sGCβ_1 was high.

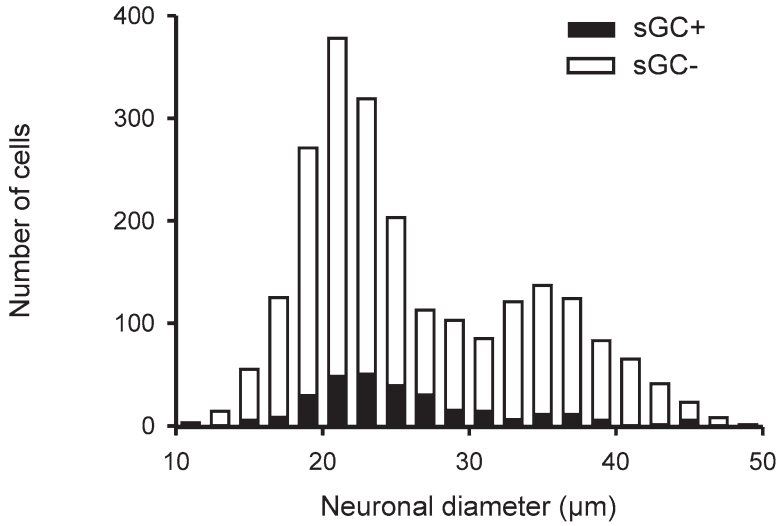

Fig. 5. Size distribution of sGCβ_1-expressing DRG cells. The size distribution was determined by measuring the diameter of sGCβ_1-positive and -negative neurons in DRGs from three animals (a total of 2273 cells counted). The total height of the bars reflects the total DRG population and shows the characteristic bimodal size distribution of DRG neurons. sGCβ_1-expressing neurons are found predominantly among the small- and medium-sized neurons.

were not able to detect a specific neuronal eNOS staining in the DRG.

Similar to the results in spinal cord, iNOS-ir was found only in laminar, vasculature-associated structures (Fig. 4E).

sGCβ_1 is expressed in a subpopulation of small, SP-containing DRG neurons

Using the sGCβ_1 antibody #1, only satellite cells were stained in DRGs (not shown). In contrast, the sGCβ_1 antibody #2 revealed sGCβ_1-ir both in satellite cells and in neurons. Only strongly labeled neurons were considered as immunopositive (Fig. 4F). In total, 12±1% of lumbar DRG neurons were strongly stained for sGCβ_1 (853–973 cells examined per animal, $n=3$ rats). The size distribution showed that mostly small or medium-sized, but also some large neurons exhibited sGCβ_1-ir (Fig. 5). Most sGCβ_1-positive neurons also exhibited SP-ir (Fig. 4F, G, 90±2%, 93–99 cells evaluated per animal, $n=3$ rats).

DISCUSSION

This study provides a detailed immunohistochemical analysis of the distribution of the different isoforms of the NO synthesizing enzyme NOS and the NO-receptor sGC in DRGs and spinal cord, including lamina I projection neurons. The results are summarized in Fig. 6 and show that while nNOS expression was scarce in lumbar spinal lamina I and DRGs, sGCβ_1 was widely expressed.

NOS immunoreactivities in spinal cord and DRGs

A previous study reported that spino-PAG neurons of adult rats do not express nNOS (Kayalioglu et al., 1999). We confirmed this result in young rat lamina I spino-PAG neurons, and found that lamina I spino-parabrachial neurons are also devoid of nNOS-ir. These results seem reliable as the overall spinal nNOS immunostaining corresponded to previous studies (Valtschanoff et al., 1992; Saito et al., 1994), and we corroborated them by NADPH

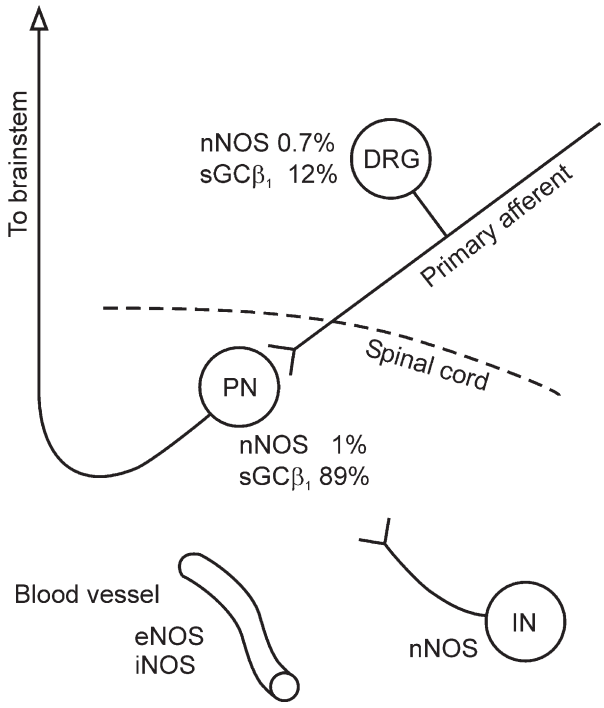

Fig. 6. Summary of results. There was very little NOS-ir located directly at the synapse between primary afferents and lamina I spino-PAG projection neurons (PN), suggesting that NO acting at this synapse comes from neighboring nNOS-ir interneurons (IN, mostly located in laminae II or III) or eNOS/iNOS-ir blood vessels. sGCβ_1 was widespread in lamina I neurons, including spino-PAG neurons, and also present in a significant proportion of primary afferents. Percentages given are percent of neurons positive for the respective antigen among DRG neurons or lamina I spino-PAG neurons.

diaphorase staining. In the DRG, we found few (0.7%) but strongly stained nNOS-ir neurons, as previously reported for lumbar DRGs (Aimi et al., 1991; Zhang et al., 1993). Most of these neurons probably had nociceptive C-fiber axons, as shown by coexpression of the marker SP (Lawson, 2002).

It has been proposed that hippocampal LTP is dependent on neuronal eNOS (O'Dell et al., 1994), and eNOS expressed in primary afferents after a nerve injury seems to play a role in neuropathic pain (Levy et al., 2000). We found no eNOS-ir neurons in spinal cord. This is in line with previous studies, where eNOS-ir in spinal cord was restricted to vascular endothelium and/or astrocytes (Phul and Smith, 2000; Kim et al., 2000; Tao et al., 2004). Regarding eNOS expression in primary afferents, previous results are contradictory. eNOS-ir was found in injured but not in healthy peripheral nerve (Levy et al., 2000). In normal DRGs, some groups localized eNOS-ir only in the vascular endothelium (Zochodne et al., 2000; Keilhoff et al., 2002), but others reported that virtually every DRG neuron expresses eNOS (Henrich et al., 2002). We found eNOS in the vasculature, which proves that the antibody detected eNOS in our hands. However, we did not find eNOS in DRG neurons either with our protocol or with the protocol used by Henrich et al. (2002). However, immunohistochemistry has a limited sensitivity, and Henrich et al. (2002) confirmed their results by single-cell PCR. Thus, one cannot exclude the presence of low levels of eNOS in DRG neurons.

In spinal cord, we found iNOS-ir around the central canal and in laminar vasculature-associated structures as previously reported (Wu et al., 1998; Xu et al., 2001). The DRGs have been found to be devoid of iNOS-ir in normal rodents (Zochodne et al., 2000; Henrich et al., 2002; Keilhoff et al., 2002), but we detected some iNOS-ir in the vasculature, like in the spinal cord. Altogether, the expression of iNOS in spinal cord and DRGs under physiological conditions is weak. However, it is known that iNOS is strongly induced in the course of peripheral inflammation (Maihöfner et al., 2000; Wu et al., 2001), explaining how it can play an important role in the generation of inflammatory pain (Osborne and Coderre, 1999).

sGCβ_1-ir in spinal cord and DRGs

sGC-mediated cGMP synthesis is a major target of NO in the nervous system (Esplugues, 2002). sGC is a heterodimer molecule consisting of an α (α1 or α2) and a β (β1 or β2) subunit. The α_1/β_1 and α_2/β_1 enzymes are widespread in the nervous system, while the expression of β_2 seems to be very low (Gibb and Garthwaite, 2001; Nedvetsky et al., 2002). We therefore chose antibodies against the β_1 subunit to detect sGC.

An sGC antibody of unknown subunit specificity stains only fibers in mouse spinal cord (Maihöfner et al., 2000), but NO induces cGMP-ir in rat spinal fibers and cell bodies (Vles et al., 2000), and very recently, lamina I neurons that have the NK1 receptor and superficial dorsal horn interneurons have been reported to express sGC (Ding and Weinberg, 2006). Consistently, we found sGCβ_1-ir in neuronal processes and somata of all laminae using antibody #1. We saw no neuronal sGCβ_1-ir with antibody #2, that also reveals no spinal sGCβ1 in Western blot (Tao and Johns, 2002). Curiously, the inverse situation was encountered in the DRGs. While both sGCβ_1 antibodies stained satellite cells, only antibody #2 also stained neurons. The two antibodies recognize different epitopes of the β_1 subunit (antibody #1 is directed against residues 593–614 and antibody #2 is directed against residues 188–207), but bind to the same protein in brain homogenates (Ding et al., 2004). The present results suggest that this may not be the case in spinal cord and peripheral nerves.

Previous evidence suggested the presence of sGC in DRGs. While in some studies NO-stimulated cGMP synthesis was limited to satellite cells (Shi et al., 1998; Thippeswamy and Morris, 2001), others found cGMP-ir also in some DRG neurons (Qian et al., 1996). Kummer et al. (1996) reported that sGCβ_2- and -α_2-ir may be localized to large ganglion cells, although these results need further study. Small- and medium-sized, SP-expressing ganglion cells contain one of the cGMP targets, cGMP-dependent protein kinase I (Qian et al., 1996). We found sGCβ_1-ir in a small subgroup of ganglion cells that were also immunopositive for SP, and therefore most of them probably were nociceptive C-fibers (Lawson, 2002). Primary afferent C-fiber terminals in the superficial dorsal horn only rarely express sGC (Ding and Weinberg, 2006).

cGMP-ir in spinal cord

Presence of the sGCβ_1 subunit does not necessarily mean presence of functional sGC. We used cGMP immunohistochemistry to detect active sGC. After stimulation with a concentration of the NO-donor SNAP that should be supramaximal for activation of sGC (de Saram et al., 2002; Garthwaite, 2005), only 35% of the lamina I projection neurons showed cGMP-ir in the soma as opposed to 89% that expressed sCGβ_1. This could mean that in some neurons the sGC subunits are assembled only in the neuronal processes, e.g. in synaptic contacts to primary afferent C-fibers, or not assembled at all. A dense network of dorsal horn neuronal fibers exhibited cGMP-ir after treatment with SNAP, as reported previously (Vles et al., 2000).

Differences and similarities between lamina I spino-PAG- and spino-parabrachial neurons

The PAG and parabrachial area are major projection targets of lamina I neurons (Todd et al., 2000). Most spino-PAG neurons have collaterals to the parabrachial area and thus they constitute a subgroup of the spino-parabrachial neurons, allegedly accounting for about 30% of them (Spike et al., 2003). However, both immunohistochemical and electrophysiological data suggest that spino-PAG neurons represent a distinct subclass of lamina I projection neurons. Compared with spino-parabrachial neurons, they show different levels of NK1 receptor-ir, specific firing patterns and afterpotentials, and a larger action-potential-independent excitatory input (Spike et al., 2003; Ruscheweyh et al., 2004; Dahlhaus et al., 2005). In addition,

while spino-PAG neurons express LTP at their synapses with primary afferent C-fibers only in response to a low frequency conditioning stimulation, spino-parabrachial neurons do so exclusively after a high frequency stimulation. We have recently shown that in contrast to the LTP at spino-PAG neurons, the LTP at spino-parabrachial neurons is not dependent on NO (Ikeda et al., in press). In the present study, we found that the distribution of NOS and sGCβ_1 was comparable in spino-PAG and spino-parabrachial neurons, and similar levels of NO-stimulated cGMP expression showed that the NO-sensing machinery was functional in (at least part of) both types of projection neurons. The different NO-sensitivity of their LTP could thus lie either in different signal transduction pathways downstream from cGMP or in the release of different amounts of NO in response low-frequency and high-frequency stimulation. It was beyond the scope of this paper to investigate these possibilities.

Possible sources and sites of action of NO in chronic pain and spinal LTP

NO production by spinal nNOS and iNOS and upregulation of these enzymes in neurons and/or glia are involved in inflammatory and neuropathic pain (Zhang et al., 1993; Meller and Gebhart, 1993; Osborne and Coderre, 1999; Maihöfner et al., 2000; Wu et al., 2001). One possible role for NO in chronic pain could be a contribution to spinal amplification of nociceptive information, e.g. by enabling or enhancing synaptic LTP at NK1 receptor-expressing lamina I projection neurons. Indeed, *in vitro* experiments have shown that the LTP between primary afferent C-fibers and lamina I neurons with a projection to the PAG is NO-dependent (Ikeda et al., in press). Importantly, spinal C-fiber-mediated LTP *in vivo* is also NO-dependent (Zhang et al., 2005; Ikeda et al., in press).

In hippocampal LTP, NO acts as a retrograde messenger, diffusing from the postsynaptic cell to the presynaptic terminal (Hawkins et al., 1998). This seems not a likely possibility for the LTP at spino-PAG neurons because their somata did not show NOS-ir, although with our methods we cannot exclude the presence of NOS in dendritic processes. Subject to the same limitation, anterograde transmission by nNOS-generated NO also seems unlikely because it would imply that the scarce ($<$1%) nNOS-positive primary afferents selectively contact spino-PAG neurons. However, the results of Henrich et al. (2002) suggest that anterograde transmission by eNOS-generated NO might be a possibility. Both spino-PAG neurons and a small subgroup of primary afferent C-fibers had the β_1 subunit of the NO-receptor sGC, and at least a portion of the spino-PAG neurons responded to exogenously applied NO with a measurable cGMP synthesis in the soma. Thus, from our data the most probable scenario is that the NO necessary for LTP induction comes from a source not directly related to the synapse between C-fiber and spino-PAG neuron, similar to what has been described in cerebellar synaptic plasticity (Daniel et al., 1998). NO can diffuse over several tens of micrometers (Wood and Garthwaite, 1994). It could thus be produced by the nNOS-expressing neurons in laminae II and III, their processes in lamina I and III, or by eNOS/iNOS-expressing blood vessels. From there, it would diffuse to the synapse that is undergoing LTP, where the spino-PAG neuron and perhaps the C-fiber terminal would be possible targets (Fig. 6).

Acknowledgments—The authors wish to thank Dr. Jan de Vente for providing the cGMP antibody and for very helpful discussions. We further thank Dr. Harald H. H. W. Schmidt for providing one of the sGC antibodies and Dr. Alain Burette for advise with the sGC immunohistochemistry.

This work was supported by the Jubiläumsfonds der Österreichischen Nationalbank (Austria) and the Austrian Science Fund (FWF). The work of A.S. was supported by a DFG grant (SFB488/A6).

REFERENCES

Aimi Y, Fujimura M, Vincent SR, Kimura H (1991) Localization of NADPH-diaphorase-containing neurons in sensory ganglia of the rat. J Comp Neurol 306:382–392.

Constantine-Paton M, Cline HT (1998) LTP and activity-dependent synaptogenesis: the more alike they are, the more different they become. Curr Opin Neurobiol 8:139–148.

Dahlhaus A, Ruscheweyh R, Sandkühler J (2005) Synaptic input of rat spinal lamina I projection and unidentified neurons *in vitro*. J Physiol 566:355–368.

Daniel H, Lévénès C, Crépel F (1998) Cellular mechanisms of cerebellar LTD. Trends Neurosci 21:401–407.

de Saram K, McNeill KL, Khokher S, Ritter JM, Chowienczyk PJ (2002) Divergent effects of vitamin C on relaxations of rabbit aortic rings to acetylcholine and NO-donors. Br J Pharmacol 135: 1044–1050.

de Vente J, Hopkins DA, Markerink-van Ittersum M, Emson PC, Schmidt HH, Steinbusch HW (1998) Distribution of nitric oxide synthase and nitric oxide-receptive, cyclic GMP-producing structures in the rat brain. Neuroscience 87:207–241.

Ding JD, Burette A, Nedvetsky PI, Schmidt HH, Weinberg RJ (2004) Distribution of soluble guanylyl cyclase in the rat brain. J Comp Neurol 472:437–448.

Ding JD, Weinberg RJ (2006) Localization of soluble guanylyl cyclase in the superficial dorsal horn. J Comp Neurol 495:668–678.

Ding Y-Q, Takada M, Shigemoto R, Mizuno N (1995) Spinoparabrachial tract neurons showing substance P receptor-like immunoreactivity in the lumbar spinal cord of the rat. Brain Res 674:336–340.

Esplugues JV (2002) NO as a signalling molecule in the nervous system. Br J Pharmacol 135:1079–1095.

Garthwaite J (2005) Dynamics of cellular NO-cGMP signaling. Front Biosci 10:1868–1880.

Gibb BJ, Garthwaite J (2001) Subunits of the nitric oxide receptor, soluble guanylyl cyclase, expressed in rat brain. Eur J Neurosci 13:539–544.

Hawkins RD, Son H, Arancio O (1998) Nitric oxide as a retrograde messenger during long-term potentiation in hippocampus. Prog Brain Res 118:155–172.

Henrich M, Hoffmann K, König P, Gruss M, Fischbach T, Gödecke A, Hempelmann G, Kummer W (2002) Sensory neurons respond to hypoxia with NO production associated with mitochondria. Mol Cell Neurosci 20:307–322.

Hoheisel U, Unger T, Mense S (2005) The possible role of the NO-cGMP pathway in nociception: Different spinal and supraspinal action of enzyme blockers on rat dorsal horn neurones. Pain 117:358–367.

Hu WH, Qiang WA, Li F, Liu N, Wang GQ, Wang HY, Wan XS, Liao WH, Liu JS, Jen MF (2000) Constitutive and inducible nitric oxide synthases after dynorphin-induced spinal cord injury. J Chem Neuroanat 17:183–197.

Ikeda H, Heinke B, Ruscheweyh R, Sandkühler J (2003) Synaptic plasticity in spinal lamina I projection neurons that mediate hyperalgesia. Science 299:1237–1240.

Ikeda H, Murase K (2004) Glial nitric oxide-mediated long-term presynaptic facilitation revealed by optical imaging in rat spinal dorsal horn. J Neurosci 24:9888–9896.

Ikeda H, Stark J, Fischer H, Wagner M, Drdla R, Jäger T, Sandkühler J (2006) Synaptic amplifier of inflammatory pain in the spinal dorsal horn. Science, in press.

Kayalioglu G, Robertson B, Kristensson K, Grant G (1999) Nitric oxide synthase and interferon-gamma receptor immunoreactivities in relation to ascending spinal pathways to thalamus, hypothalamus, and the periaqueductal grey in the rat. Somatosens Mot Res 16: 280–290.

Keilhoff G, Fansa H, Wolf G (2002) Neuronal nitric oxide synthase is the dominant nitric oxide supplier for the survival of dorsal root ganglia after peripheral nerve axotomy. J Chem Neuroanat 24: 181–187.

Khasabov SG, Rogers SD, Ghilardi JR, Peters CM, Mantyh PW, Simone DA (2002) Spinal neurons that possess the substance P receptor are required for the development of central sensitization. J Neurosci 22:9086–9098.

Kim S, Moon C, Wie MB, Kim H, Tanuma N, Matsumoto Y, Shin T (2000) Enhanced expression of constitutive and inducible forms of nitric oxide synthase in autoimmune encephalomyelitis. J Vet Sci 1:11–17.

Kummer W, Behrends S, Schwarzlmüller T, Fischer A, Koesling D (1996) Subunits of soluble guanylyl cyclase in rat and guinea-pig sensory ganglia. Brain Res 721:191–195.

Lawson SN (2002) Phenotype and function of somatic primary afferent nociceptive neurones with C-, Aδ- or Aα/β-fibres. Exp Physiol 87: 239–244.

Levy D, Tal M, Hoke A, Zochodne DW (2000) Transient action of the endothelial constitutive nitric oxide synthase (ecNOS) mediates the development of thermal hypersensitivity following peripheral nerve injury. Eur J Neurosci 12:2323–2332.

Maihöfner C, Euchenhofer C, Tegeder I, Beck KF, Pfeilschifter J, Geisslinger G (2000) Regulation and immunohistochemical localization of nitric oxide synthases and soluble guanylyl cyclase in mouse spinal cord following nociceptive stimulation. Neurosci Lett 290:71–75.

Mantyh PW, Rogers SD, Honoré P, Allen BJ, Ghilardi JR, Li J, Daughters RS, Lappi DA, Wiley RG, Simone DA (1997) Inhibition of hyperalgesia by ablation of lamina I spinal neurons expressing the substance P receptor. Science 278:275–279.

Meller ST, Gebhart GF (1993) Nitric oxide (NO) and nociceptive processing in the spinal cord. Pain 52:127–136.

Nedvetsky PI, Kleinschnitz C, Schmidt HH (2002) Regional distribution of protein and activity of the nitric oxide receptor, soluble guanylyl cyclase, in rat brain suggests multiple mechanisms of regulation. Brain Res 950:148–154.

Nichols ML, Allen BJ, Rogers SD, Ghilardi JR, Honoré P, Luger NM, Finke MP, Li J, Lappi DA, Simone DA, Mantyh PW (1999) Transmission of chronic nociception by spinal neurons expressing the substance P receptor. Science 286:1558–1561.

O'Dell TJ, Huang PL, Dawson TM, Dinerman JL, Snyder SH, Kandel ER, Fishman MC (1994) Endothelial NOS and the blockade of LTP by NOS inhibitors in mice lacking neuronal NOS. Science 265: 542–546.

Osborne MG, Coderre TJ (1999) Effects of intrathecal administration of nitric oxide synthase inhibitors on carrageenan-induced thermal hyperalgesia. Br J Pharmacol 126:1840–1846.

Phul RK, Smith ME (2000) Expression of nitric oxide synthase in the spinal cord in C57BL/6J mice with congenital muscular dystrophy. Muscle Nerve 23:63–72.

Qian Y, Chao DS, Santillano DR, Cornwell TL, Nairn AC, Greengard P, Lincoln TM, Bredt DS (1996) cGMP-dependent protein kinase in dorsal root ganglion: relationship with nitric oxide synthase and nociceptive neurons. J Neurosci 16:3130–3138.

Ruscheweyh R, Ikeda H, Heinke B, Sandkühler J (2004) Distinctive membrane and discharge properties of rat spinal lamina I projection neurones *in vitro*. J Physiol 555:527–543.

Saito S, Kidd GJ, Trapp BD, Dawson TM, Bredt DS, Wilson DA, Traystman RJ, Snyder SH, Hanley DF (1994) Rat spinal cord neurons contain nitric oxide synthase. Neuroscience 59:447–456.

Sandkühler J (2000) Learning and memory in pain pathways. Pain 88:113–118.

Shi TJ, Holmberg K, Xu ZQ, Steinbusch H, de Vente J, Hökfelt T (1998) Effect of peripheral nerve injury on cGMP and nitric oxide synthase levels in rat dorsal root ganglia: time course and coexistence. Pain 78:171–180.

Spike RC, Puskár Z, Andrew D, Todd AJ (2003) A quantitative and morphological study of projection neurons in lamina I of the rat lumbar spinal cord. Eur J Neurosci 18:2433–2448.

Swanson LW (1992) Brain maps: structure of the rat brain. Amsterdam: Elsevier.

Tanaka J, Markerink-van Ittersum M, Steinbusch HW, de Vente J (1997) Nitric oxide-mediated cGMP synthesis in oligodendrocytes in the developing rat brain. Glia 19:286–297.

Tao F, Tao YX, Zhao C, Dore S, Liaw WJ, Raja SN, Johns RA (2004) Differential roles of neuronal and endothelial nitric oxide synthases during carrageenan-induced inflammatory hyperalgesia. Neuroscience 128:421–430.

Tao YX, Johns RA (2002) Activation and up-regulation of spinal cord nitric oxide receptor, soluble guanylate cyclase, after formalin injection into the rat hind paw. Neuroscience 112:439–446.

Thippeswamy T, Morris R (2001) Evidence that nitric oxide-induced synthesis of cGMP occurs in a paracrine but not an autocrine fashion and that the *site* of its release can be regulated: studies in dorsal root ganglia *in vivo* and *in vitro*. Nitric Oxide 5:105–115.

Todd AJ, McGill MM, Shehab SAS (2000) Neurokinin 1 receptor expression by neurons in laminae I, III and IV of the rat spinal dorsal horn that project to the brainstem. Eur J Neurosci 12:689–700.

Töpel I, Stanarius A, Wolf G (1998) Distribution of the endothelial constitutive nitric oxide synthase in the developing rat brain: an immunohistochemical study. Brain Res 788:43–48.

Valtschanoff JG, Weinberg RJ, Rustioni A (1992) NADPH diaphorase in the spinal cord of rats. J Comp Neurol 321:209–222.

Vles JS, de Louw AJ, Steinbusch H, Markerink-van Ittersum M, Steinbusch HW, Blanco CE, Axer H, Troost J, de Vente J (2000) Localization and age-related changes of nitric oxide- and ANP-mediated cyclic-GMP synthesis in rat cervical spinal cord: an immunocytochemical study. Brain Res 857:219–234.

Wood J, Garthwaite J (1994) Models of the diffusional spread of nitric oxide: implications for neural nitric oxide signalling and its pharmacological properties. Neuropharmacology 33:1235–1244.

Wu J, Fang L, Lin Q, Willis WD Jr (2001) Nitric oxide synthase in spinal cord central sensitization following intradermal injection of capsaicin. Pain 94:47–58.

Wu J, Lin Q, Lu Y, Willis WD Jr, Westlund KN (1998) Changes in nitric oxide synthase isoforms in the spinal cord of rat following induction of chronic arthritis. Exp Brain Res 118:457–465.

Xu J, Kim GM, Chen S, Yan P, Ahmed SH, Ku G, Beckman JS, Xu XM, Hsu CY (2001) iNOS and nitrotyrosine expression after spinal cord injury. J Neurotrauma 18:523–532.

Zabel U, Häusler C, Weeger M, Schmidt HH (1999) Homodimerization of soluble guanylyl cyclase subunits. Dimerization analysis using a glutathione *S*-transferase affinity tag. J Biol Chem 274:18149–18152.

Zabel U, Weeger M, La M, Schmidt HH (1998) Human soluble guanylate cyclase: functional expression and revised isoenzyme family. Biochem J 335:51–57.

Zhang X, Verge VMK, Wiesenfeld-Hallin Z, Ju G, Bredt D, Synder SH, Hökfelt T (1993) Nitric oxide synthase-like immunoreactivity in lumbar dorsal root ganglia and spinal cord of rat and monkey and effect of peripheral axotomy. J Comp Neurol 335:563–575.

Zhang XC, Zhang YQ, Zhao ZQ (2005) Involvement of nitric oxide in long-term potentiation of spinal nociceptive responses in rats. Neuroreport 16:1197–1201.

Zochodne DW, Verge VMK, Cheng C, Hoke A, Jolley C, Thomsen K, Rubin I, Lauritzen M (2000) Nitric oxide synthase activity and expression in experimental diabetic neuropathy. J Neuropathol Exp Neurol 59:798–807.

(Accepted 4 April 2006)
(Available online 24 May 2006)